Chemistry & Biology, Vol. 12, 329–337, March, 2005, ©2005 Elsevier Ltd All rights reserved. DOI 10.1016/j.chembiol.2005.01.012

Identification of Amino Acids that Promote Specific and Rigid TAR RNA-Tat Protein Complex Formation

Thomas E. Edwards,[1] Bruce H. Robinson,[1] and Snorri Th. Sigurdsson[1,2,*]
[1]Department of Chemistry
University of Washington
Seattle, Washington 98195
[2]University of Iceland
Science Institute, Dunhaga 3
107 Reykjavík
Iceland

Summary

The Tat protein and the transactivation responsive (TAR) RNA form an essential complex in the HIV lifecycle, and mutations in the basic region of the Tat protein alter this RNA-protein molecular recognition. Here, EPR spectroscopy was used to identify amino acids, flanking an essential arginine of the Tat protein, which contribute to specific and rigid TAR-Tat complex formation by monitoring changes in the mobility of nitroxide spin-labeled TAR RNA nucleotides upon binding. Arginine to lysine N-terminal mutations did not affect TAR RNA interfacial dynamics. In contrast, C-terminal point mutations, R56 in particular, affected the mobility of nucleotides U23 and U38, which are involved in a base-triple interaction in the complex. This report highlights the role of dynamics in specific molecular complex formation and demonstrates the ability of EPR spectroscopy to study interfacial dynamics of macromolecular complexes.

Introduction

The transactivation responsive (TAR) RNA is the 5′-leader sequence of the HIV-1 mRNA genome and interacts with the Tat protein during transcription [1]. TAR and Tat bind to cyclin T1 (CycT1) and cyclin-dependent kinase 9 (CDK9) as part of the positive transcription elongation factor (P-TEFb) complex to counter the effect of negative elongation factors [2] and promote efficient transcription of the full-length HIV genome [3]. In the absence of the TAR-Tat interaction, viral transcription is inefficient [4], which makes the TAR RNA-Tat protein complex an important target for therapeutic intervention of HIV replication [5, 6].

A duplex stem containing a trinucleotide bulge has been identified as the Tat binding region of the TAR RNA (Figure 1A) by numerous studies utilizing electrophoretic mobility shift assays to examine the effect of RNA mutagenesis on complex formation [7–12]. The basic domain of the Tat protein spanning residues 47–57 has been identified as the TAR RNA binding region in a similar manner [7, 8, 13, 14]. In particular, arginine 52 (R52) has been identified as a critical amino acid for TAR-Tat complex formation [15–17]. Mutation of several residues flanking R52 to lysine resulted in minimal loss of either binding affinity for short Tat-derived peptides [15, 17, 18] or transactivation activity for the full Tat protein [14, 15, 17, 18], signifying that only R52 is essential for complex formation.

Despite extensive efforts, a high-resolution structure of the HIV TAR-Tat complex has not been obtained. However, the NMR solution structures of the TAR RNA [19] and the Tat protein [20–22] have been solved individually. Several NMR studies have investigated the TAR RNA structural change that takes place upon binding to derivatives of the Tat protein such as arginine [23, 24], argininamide [25–28] or Tat-derived peptides [19, 29]. These studies have revealed two levels of molecular recognition that include specific and nonspecific complex formation [29]. In particular, imino proton NMR spectroscopic data indicated that a specific complex was formed in the presence of the wild-type peptide containing the core sequence RKKRRQRRR (residues 49–57), whereas the markers for specific complex formation were absent in the presence of a mutant peptide containing the core sequence RKKRKQKKK [29].

Incorporation of nitroxide spin-labels enables investigation of internal motions and ligand-induced conformational changes using electron paramagnetic resonance (EPR) spectroscopy [30–33]. Recently, we used EPR spectroscopy to examine the binding of argininamide, a mutant Tat-derived peptide (YKKKKRKKKKA), and a wild-type peptide (YGRKKRRQRRR, residues 47–57) to nitroxide spin-labeled TAR RNAs [34]. As expected, similar overall changes in RNA internal dynamics were observed for the three Tat derivatives upon complex formation, indicating similar structural changes in the RNA upon binding. However, significantly larger decreases in mobility at U23 and U38 were observed in the presence of the wild-type peptide in comparison with argininamide or mutant peptide binding. Hence, both EPR and NMR spectroscopy [29] indicate that in addition to arginine 52, amino acids present in the wild-type peptide that are not present in the mutant peptide are responsible for the increased specificity in molecular recognition.

Although there is substantial evidence for the participation of the amino acids flanking the essential arginine 52 in formation of the rigid complex, the structural role of individual amino acids in the flanking regions has not been identified. One reason is that it is not possible to measure the contribution of individual amino acids toward TAR-Tat complex formation by traditional mutagenesis and binding assays due to the similar binding affinities of the mutant and wild-type Tat-derived peptides. It is possible to use solution NMR spectroscopy of isotopically labeled RNA, but screening individual amino acids would be costly and labor intensive. In contrast, EPR spectroscopy only requires small quantities of material (0.1–2 nmol per sample), has short data acquisition times (typically 1–2 hr per sample), and is sensitive to variations in RNA structure and internal dynamics upon binding to different ligands [35, 36]. Therefore, EPR spectroscopy of site specifically spin-labeled RNA offers an efficient method for identifying

*Correspondence: snorrisi@hi.is

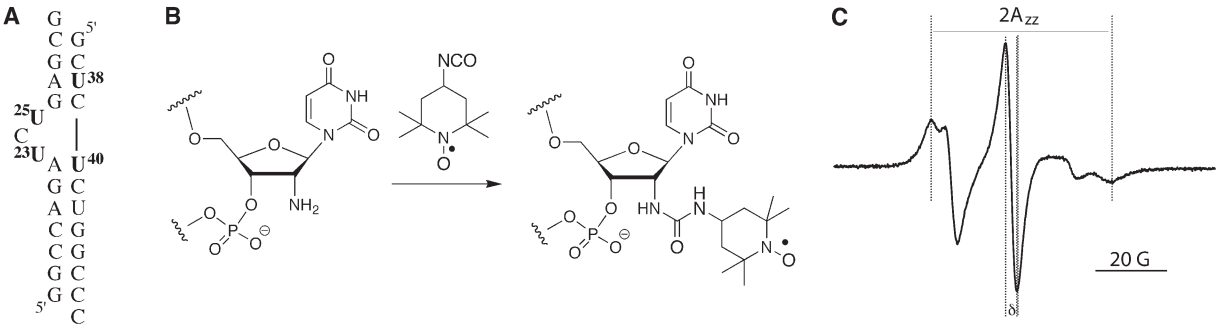

Figure 1. Applying EPR Spectroscopy to the TAR RNA

(A) Construct of the TAR RNA used in this study with spin-labeling sites indicated in bold.
(B) Preparation of spin-labeled RNA.
(C) EPR spectrum of U23 TAR in the absence of peptide with EPR spectral width ($2A_{zz}$) and centerline width (δ) indicated.

amino acids responsible for rigid RNA-protein complex formation.

Here, we describe the use of EPR spectroscopy to determine which amino acids in the basic region of the Tat protein are responsible for the observed decreases in U23 and U38 mobility in the wild-type TAR RNA-Tat peptide complex. Changes in nitroxide spin-label mobility, which have been shown to correlate with differences in nucleotide mobility [37], were investigated at four RNA sites upon incubation with a series of Tat-derived mutant peptides. Our results indicate that mutations in the C-terminal end of the Tat basic region, but not the N-terminal end, interfere with wild-type RNA dynamics in the TAR-Tat complex, and that specifically, arginine 56 most prominently contributes to U38 immobilization. These results are presented in the context of known structural and transcriptional data.

Results

Experimental Design

Recently, we developed a general and efficient method to site specifically incorporate nitroxide spin-labels into nucleic acids [37] in order to facilitate the study of ligand-induced RNA conformational changes by EPR spectroscopy [33–36, 38–40] in a manner analogous to studies currently being performed for proteins [41–44]. Four TAR RNAs were prepared such that each contained a nitroxide spin-labeled nucleoside within the Tat binding region (Figure 1). We previously showed that spin-labels at these sites have little effect on TAR-Tat binding affinity by native gel electrophoresis [34]. In addition, titration of the Tat wild-type peptide to U40 spin-labeled RNA revealed changes in the EPR spectral width up to 1 equivalent of peptide (0.2 mM), after which no further changes were observed until line broadening was observed at 0.7 mM concentration of peptide. These results indicate complete and specific binding at the lower peptide concentrations, but non-specific binding or aggregation at higher peptide concentrations [34]. In the current study, a series of peptides were designed to test the influence of amino acids in the basic region of the Tat protein on rigid TAR-Tat molecular recognition (Figure 2). Given the sequences of the wild-type and Tat I peptides, candidate amino acids that could provide the observed increase in specificity [34] are glycine 48, arginines 49, 53, 55, 56, and 57 and glutamine 54. Peptide II was designed to test the influence of residues on the N-terminal end, whereas peptides III and IV were designed to test the contribution of amino acids on the C-terminal end. In addition, peptides V, VI, VII, and VIII were prepared to test the influence of single arginines at C-terminal residues 53, 55, 56, and 57, respectively, by mutation to lysine. In the presence of these peptides, changes in U25 mobility were similar to those previously observed [34] showing TAR-Tat complex formation with the mutant peptides (Figure 3). In addition, changes in U40 mobility were also consistent with previous results [34], although peptides II–VIII resulted in increased spectral width (2–5 G) relative to the wild-type peptide (Figure 3). However, no clear trends emerged among these mutants, and thus these minor differences were not investigated further.

EPR Spectral Analysis

Typically, three types of motion can be studied by EPR spectroscopy [32]. First, the probe can move indepen-

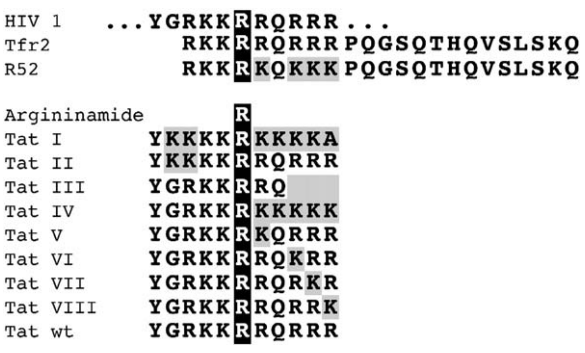

Figure 2. Sequence Analysis of Tat Protein Derivatives

Multiple sequence alignment of wild-type HIV-1 protein; the Tat-derived peptides used by Long and Crothers, Tfr24 and R52 [29]; and the Tat-derived peptides used for the EPR spectroscopic studies.

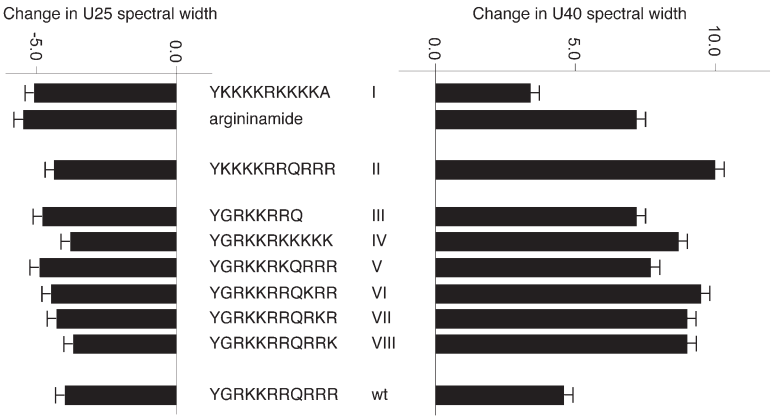

Figure 3. U25 and U40 EPR Spectroscopy of TAR RNA-Tat Peptide Complexes

Changes in EPR spectral width ($\Delta 2A_{zz}$ in gauss, G) of U25 or U40 spin-labeled TAR RNA upon binding to derivatives of the Tat protein. The approximate error in the spectral width is 0.3 G. Spectra were obtained at 0°C in 20% sucrose/100 mM NaCl, 10 mM sodium phosphate, and 0.1 mM Na_2EDTA (pH 7.0).

dent of the macromolecule. For the current study, we employed a semiflexible ureido tether, designed to minimize the motions of the probe independent of the nucleic acid [37]. Second, the global motion, arising from either the tumbling of the whole macromolecule or motions of its individual domains relative to one another can be detected. The global motion can often be eliminated by addition of sucrose to the solution; here, experimental conditions were selected to contain 20% sucrose, which largely eliminates the global motions of the macromolecular complex. The third type of motion is the local motion, which in our case would be the motion of the nucleotide to which the probe is attached. Although steps have been taken to minimize the first two types of motion to allow us to study the local motion of the TAR RNA, a component of the overall observed motion probably originates from movement of the probe independent of the nucleic acid and/or movement of individual domains within the RNA or RNA-protein complex.

Incorporation of a nitroxide spin-label via a 2′-ureido linkage allows for the detection of structure-dependent dynamics by EPR spectroscopy [37]. Specifically, nitroxides located at flexible positions such as U23 and U25 exhibit narrower spectral widths, which correlate with increased motion of the nitroxide spin-probe [45], relative to those in base-paired sites (U38 and U40) [37]. For the current study, changes in EPR spectral width ($\Delta 2A_{zz}$) upon complex formation were plotted for each nucleotide as a function of peptide mutation, thus showing increased or decreased nucleotide mobility relative to the unbound TAR RNA (Figures 3–5). Alternatively, nitroxide motions can be monitored by determining the effective local rotational correlation times (τ_R) according to the ΔS method [45], or by calculating the scaled relative mobility factor (M_s), which provides a simple semiquantitative measure of the nitroxide mobility [32] (see Supplemental Data for calculations). For each EPR spectrum presented here, values for all spectral parameters ($2A_{zz}$, τ_R, and M_s) are presented in the Supplemental Data; for the current study $2A_{zz}$ ranged from 50.5 to 72.0 G, with an error of ±0.3 G; τ_R ranged from 2.4 to 27.4 ns, with a typical error of ±0.2 ns; M_s ranged from 0.04 to 0.53, with a typical error of ±0.04 arbitrary units. These parameters for semiquantitative determination of nitroxide mobility provide essentially the same type of information; for example, plotting M_s as a function of peptide mutation (Supplemental Data) gives the same information as that presented in Figures 3–5. Thus the same conclusions are reached by monitoring the changes in the EPR spectral width ($\Delta 2A_{zz}$) as from the ΔS method or the scaled relative mobility factor (M_s). In this paper, we present our results using the EPR spectral width to monitor changes in TAR RNA nucleotide dynamics.

Mutations that Affect U23 TAR RNA Internal Dynamics

The wild-type Tat peptide induced large changes in the EPR spectrum of U23 TAR RNA ($\Delta 2A_{zz}$ = +12.5 G, τ_R = 6.1 ns, and M_s = 0.29), whereas Tat peptide I induced small changes ($\Delta 2A_{zz}$ = +0.8 G, τ_R = 2.6 ns, and M_s = 0.48) relative to U23 TAR in the unbound state ($2A_{zz}$ = 50.5 G, τ_R = 2.4 ns, and M_s = 0.53) [34]. As the EPR spectra in Figure 4 suggest, N-terminal mutations (peptide II) do not alter U23 dynamics relative to the native state. Multiple C-terminal amino acid deletions (III) or mutations (IV) moderately increase the mobility of U23 relative to the native state. On the other hand, individual C-terminal mutations induce small increases in U23 mobility, most notably at positions R53 (V), R55 (VI), and R56 (VII), although no difference was observed at position R57 (VII). Overall, mutations in the C-terminal end of the Tat peptide basic region change U23 internal dynamics to intermediate dynamic states, relative to the U23 dynamics observed for peptide I and the wild-type peptide.

Mutations that Affect U38 TAR RNA Internal Dynamics

The dynamics of U38 in the free TAR RNA closely resemble that of a typical base-paired residue in a duplex, as evident by nearly superimposable EPR spectra in comparison with U38 in a version of the TAR RNA lacking a trinucleotide bulge (i.e., a simple 12 base-pair duplex stem exactly complementary to the U38 strand; data not shown). The U38 TAR RNA dynamics are significantly decreased relative to the dynamics observed in flexible regions, with a correlation time similar to that estimated for the TAR RNA-peptide complex [37]. In comparison with Tat peptide I ($\Delta 2A_{zz}$ = +0.4 G, τ_R = 2.7 ns, and M_s = 0.38), U38 is extremely rigid in the presence of the wild-type peptide ($\Delta 2A_{zz}$ = +19.8 G, τ_R = 27.4 ns, and M_s = 0.04) and displays dynamics similar

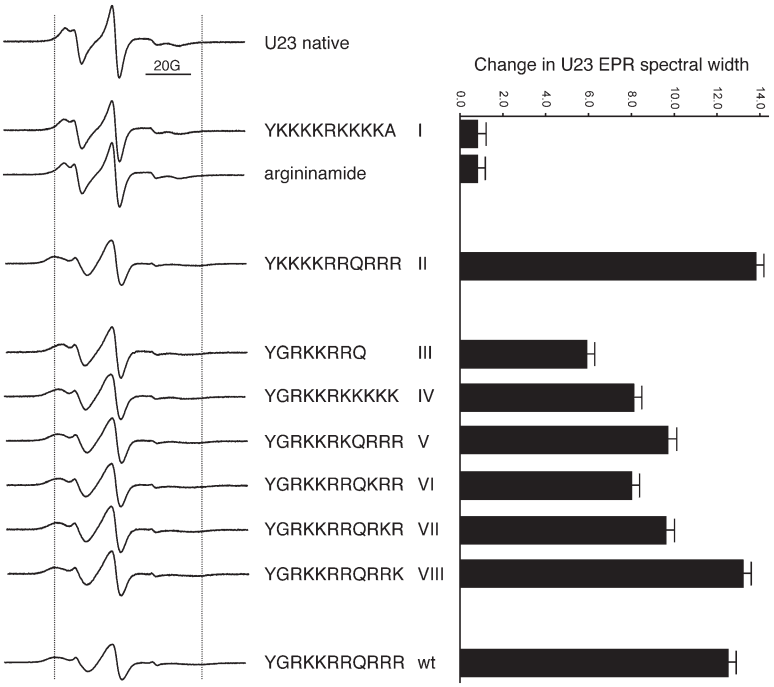

Figure 4. U23 EPR Spectroscopy of TAR RNA-Tat Peptide Complexes

EPR spectra of U23 and changes in EPR spectral width ($2A_{zz}$ in gauss, G) in the presence of Tat-derived peptides. The dotted lines indicate the spectral width of U23 in the presence of the wild-type (wt) peptide and are extended through the other spectra for visual comparison.

to the expected global dynamics of the complex [34]. Mutation of G48 and R49 to lysine in the N-terminal end of the Tat protein basic region did not affect U38 dynamics in the TAR-Tat complex (peptide II, Figure 5). Removal of the three C-terminal arginine residues (55–57, peptide III) produced EPR spectra and hence nitroxide dynamics similar to that observed for the mutant (I) state, as did mutation of the five residues on the N-terminal side of R52 to lysine (IV). Individual lysine replacement mutation at R53 (V), R55 (VI), or R57 (VII) increased U38 internal dynamics relative to the wild-type peptide. Much more dramatic was the observed mutation of R56 to lysine, which changed the mobility of the U38 spin-label to a degree similar to peptide I ($\Delta 2A_{zz}$ = +2.2 G, τ_R = 3.0 ns, and M_s = 0.26).

The U38 spectra in the presence of mutant peptides V, VI, VII, and VIII appear to contain two components (Figure 5). On first inspection, the two states closely

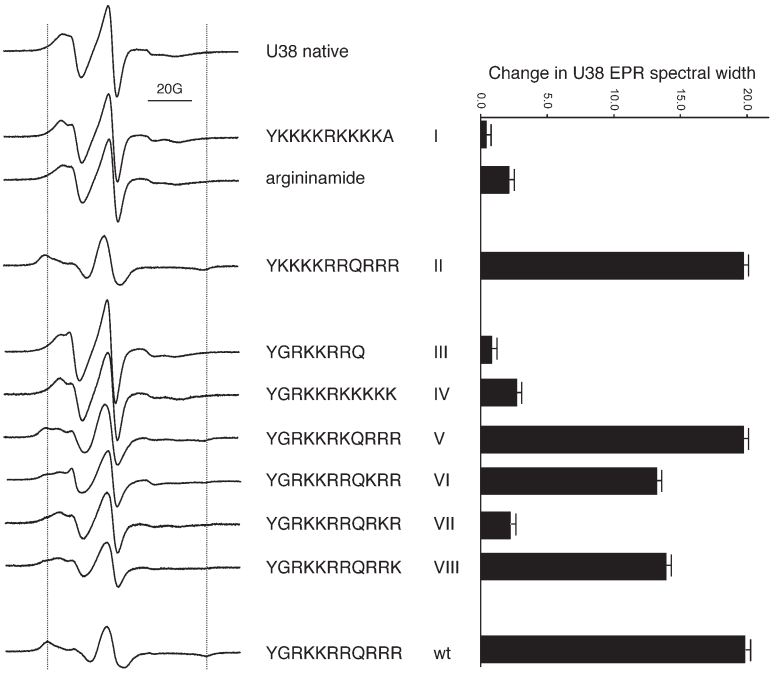

Figure 5. U38 EPR Spectroscopy of TAR RNA-Tat Peptide Complexes

EPR spectra of U38 and changes in EPR spectral width ($2A_{zz}$ in gauss, G) in the presence of Tat-derived peptides. The dotted lines indicate the spectral width of U38 in the presence of the wild-type (wt) peptide and are extended through the other spectra for visual comparison.

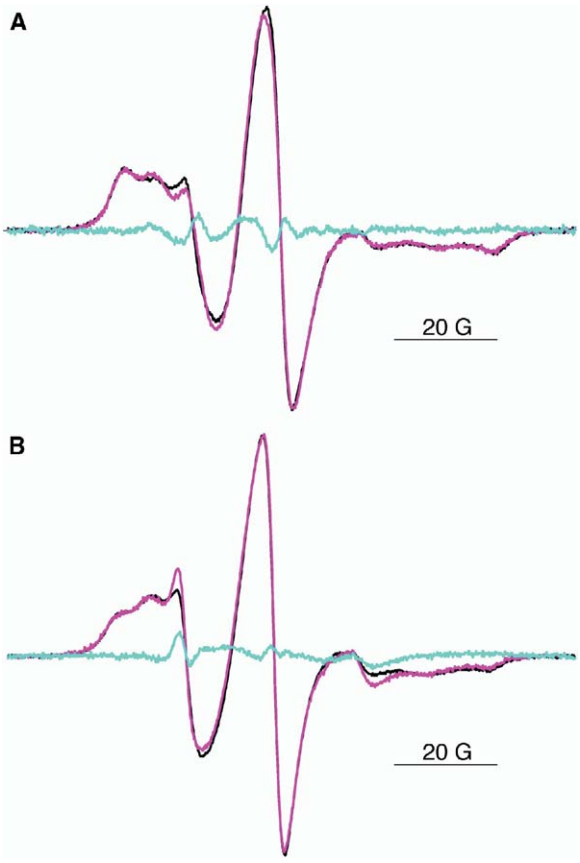

Figure 6. Spectral Fittings of U38 Multicomponent EPR Spectra

Spectral fitting of U38 EPR spectra in the presence of Tat-derived peptides V (A) and VI (B); the black spectra are the experimental spectra, the magenta spectra are the composite spectra, and the cyan spectra are the difference spectra.

resemble the rigid complex observed in the presence of the wild-type peptide and the flexible state obtained for the complex with peptide I. We tested this observation by developing a least squares optimization to fit these spectra to a two-component system containing the wild-type peptide and mutant I peptide samples as component spectra. Component spectra were summed to give the best least squares fit to the entire composite spectra. Excellent fits were obtained for peptides V and VI, as judged by the composite and difference spectra (Figure 6). The fraction of rigid component for peptide V was 68% ± 4% and the fraction of rigid component for peptide VI was 39% ± 19%. The high error rate in the fitting for peptide VI was largely due to a free spin component in this mixture. If this free spin component is disregarded, as is commonly done by spectral subtraction, the fit is excellent. The fits for VII and VIII were poor, especially in the high and low field extremes, where the line width is most sensitive to changes in dynamics; therefore, it is likely that these spectra do not represent a simple composite of the two components investigated.

Alternatively, the fractions of each component were determined using a simple algebraic solution based on the centerline width of the mutant I peptide (δ = 3.92 G) and the wild-type peptide (δ = 7.58 G), assuming a two state model. Using this method, which is naturally biased toward the more mobile component and is, therefore, less accurate than the method presented above, the following percentages of rigid component were obtained for each peptide: V, 50%; VI, 37%; VII, 22%; and VIII, 38%. Although the fittings were poor for peptide VII and VIII, the combined results of the crude fittings and algebraic solutions give a rough estimate of the percentages of rigid and mobile components in each, even if the individual components do not correspond well with the wild-type peptide and Tat peptide I.

Discussion

RNA-protein interactions play important roles throughout biological systems. Although several RNA-protein structures have been solved by NMR spectroscopy and X-ray crystallography, few studies have focused on the recognition dynamics of RNA-protein interfaces. NMR spectroscopy of ribosomal protein-rRNA, U1A-RNA, and Stuafen protein-RNA complexes (reviewed in [46]) as well as fluorescence correlation spectroscopy of the N protein-boxB interaction from bacteriophage lambda [47] have demonstrated the functional importance of RNA dynamics in RNA-protein complex assembly. Here, we present the use of EPR spectroscopy to study the interfacial dynamics of the HIV-1 TAR RNA-Tat protein complex and use observed differences in dynamics to identify which amino acids in the Tat protein contribute to RNA rigidity in the native RNA-protein complex.

The accumulation of a large field of literature investigating the HIV-1 TAR RNA-Tat protein interaction has revealed two levels of specificity in the RNA-protein molecular recognition. At the first level, the TAR RNA forms a binding pocket around a single essential arginine at position 52, as evidenced by NMR solution structures of the TAR RNA bound to arginine-based small molecules [23, 24, 26, 27, 48]. This arginine coordinates U23, which forms a base triple with A27 and U38, and stacks on A22 and along G26 while interacting with phosphates 21 and 22. TAR-arginine complex formation induces a global RNA structural change [28, 49] and alters the internal dynamics of the nucleotides surrounding the binding region of the TAR RNA [34, 50]. At this level of specificity, the changes in nucleotide mobility observed by EPR spectroscopy of the TAR-argininamide complex [34] are generally in agreement in direction and relative magnitude with changes observed by NMR spectroscopy [50]. We denote this level of specificity the flexible level, given the relative mobility of the nucleotides [34, 50].

In the second level of molecular recognition, amino acids flanking the essential arginine contribute to the specificity of the interaction. This is manifested, for example, in moderate effects on the transcription rates (up to 3-fold [15]). Furthermore, the flanking amino acids influence the interfacial dynamics and positioning of the TAR nucleotides as observed by NMR [25, 29] and EPR spectroscopy [34], particularly of U23 and U38, which are involved in a base-triple interaction that is a key feature of TAR-Tat recognition. For example, in

the presence of the wild-type peptide ("Tfr24," Figure 2), NMR analysis revealed U23 and U38 imino resonances that were either missing (U23) or at a different chemical shift (U38) in the presence of the mutant peptide ("R52," Figure 2) [29]. In addition, EPR spectroscopy revealed large changes in U23 and U38 dynamics in the presence of the wild-type peptide (Tat wt, Figure 2), but small changes in the presence of a mutant peptide (I, Figure 2) [34]. Together, the NMR and EPR data indicate large changes in the spectroscopic properties of nucleotides U23 and U38 in the presence of the wild-type peptide compared to the TAR RNA in the presence of the Tat mutant peptide. In agreement with the biophysical data, kinetic dissociation data indicated monophasic kinetics for the wild-type peptide, but biphasic kinetics for the mutant peptide, providing further evidence that these peptides bind differently to the TAR RNA [51]. We refer to this level of specificity as the rigid level, due to the substantial decreases in U23 and U38 mobility.

The series of Tat-derived peptides studied here (Figure 2) induced similar changes in mobility with only minor variation at positions U25 and U40 (Figure 3), substantial changes in mobility with moderate sensitivity to Tat amino acid modification at U23 (Figure 4), and substantial changes in mobility with high sensitivity at U38 (Figure 5). Neither U23 nor U38 is sensitive to N-terminal peptide mutation at glycine 48 or arginine 49 (peptide II), and these amino acids are likely not involved in formation of the specific and rigid complex. In contrast, dramatic effects are seen in peptides containing mutation(s) in the C-terminal end. Our results show that single arginine to lysine mutation at either R53 (V), R55 (VI), or R56 (VII) increased the mobility of both U23 and U38 relative to the rigid wild-type state (Figures 4 and 5). The most striking result was observed upon mutation at R56, which increased the internal dynamics of U38 nearly 10-fold, relative to the effect of the wild-type peptide. Thus, the R56 mutation yielded a spectrum similar to that obtained for the Tat peptide I, indicating that R56 forms key contacts in the rigid wild-type complex. Although we describe these changes in dynamics as local effects, we cannot rule out the possibility that some of the observed changes in motion arise from movement of the probe independent of the RNA or from global motions of individual domains. Regardless of the source of these motions, however, the RNA dynamics can be used as a structural indicator to identify specific amino acids that are important for the RNA-protein complex formation.

Inspection of the U38 EPR spectra reveals that peptides V and VI contain a flexible and a rigid component, each of which has similar features to peptide I and the wild-type peptide, respectively (Figure 5). In fact, the individual spectra for peptide I and the wild-type peptide can be summed to produce an excellent fit (Figure 6). For peptide V, ~70% of the sample is in the rigid complex and ~40% for peptide VI. The U38 spectra of peptides VII and VIII seem to contain a rigid and a flexible component; however, the fittings for these spectra were poor, indicating that these samples do not contain a simple mixture of the flexible and the rigid complex as was observed for peptides V and VI, but that peptides VII and VIII adopt more complex structures and dynamics. Combined, these results indicate that the arginines in the C-terminal region are important for rigid complex formation and that they act in concert to produce a rigid TAR-Tat complex.

The EPR spectroscopic results concerning rigid and flexible complex formation correlate reasonably well with data on transcriptional activation rates. Single point mutations throughout the basic region of the Tat protein only affect transcription activation rates up to 3-fold [14, 15, 17, 18], which led to the conclusion that overall charge density of the basic region was important, but that specific residues were not essential for binding [18]. On the other hand, multiple point mutations lead to severe decreases in transcriptional activation in comparison with the wild-type protein [14, 17, 18]. Therefore, it was concluded that arginine 52 was most important for binding based on an arginine walk through a poly-lysine peptide [15]. From the EPR results presented above, single point mutations at 53, 55, and 56 produced small increases in the mobility of U23, whereas multiple point mutations at these positions largely perturbed the native state dynamics; both of these results are in agreement with results from transcription activation studies. For U38 dynamics, single point mutations at 53 (V) and 55 (VI) produced a two state equilibrium between the flexible and rigid complex (Figure 6). If formation of the rigid complex is required for high-fidelity transcription activation, one might not expect a large effect of arginine to lysine mutations at positions 53 and 55, because a substantial part of the complex can access the rigid state. The largest change in U38 dynamics was observed for the R56K mutation (VII), which predominantly produced the flexible state. However, some spectral broadening was observed, indicating a less flexible component, although simulation to a two state model between the flexible and the rigid state did not give a good fit to the experimental data. Double mutation of both amino acids 55 and 56 to alanine [18] or glutamine [14] drastically reduced transcription activation (at least 15-fold in each case); however, mutation to lysine had virtually no effect on transcription activation [18]. Therefore, it would appear that the EPR results for U38, which show the strongest effect for the R56K mutation, do not directly corroborate the transcription studies. However, more recent studies in which peptides were selected in vitro to bind to the TAR RNA have revealed that peptides with an arginine residue at position 56 appear to consistently perform 2- to 3-fold better in transcription activation studies than peptides with lysine or another amino acid at this position [52, 53].

In the absence of a high-resolution structure for the TAR-Tat complex, one can only speculate about the structural origin of the dramatic effect that R56K has on the dynamics of U38. However, inspection of the NMR solution structures of the Tat protein [20–22] provides clues about the structural origins of this effect. The NMR Tat structures show some structural variation, but all demonstrate that the basic region forms one face of the protein surface (Figure 7). More specifically, this face spans residues 52–57, suggesting that these might form an RNA binding surface; furthermore, this structural element supports the observation that the N-terminal residues 48 and 49 do not contribute to rigid

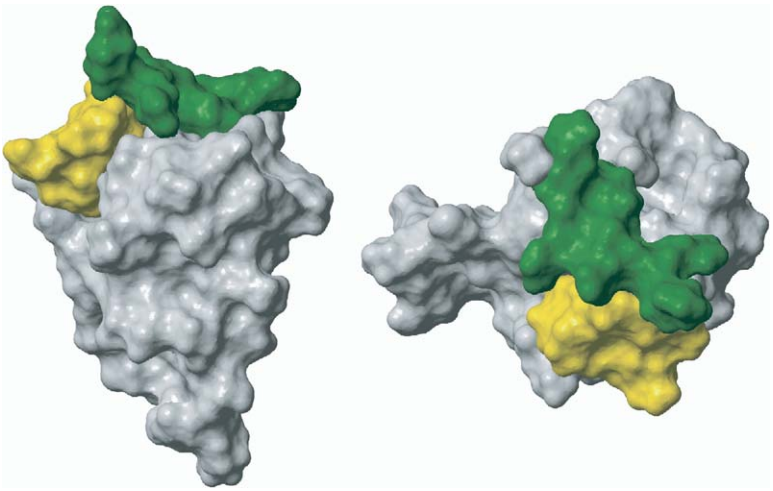

Figure 7. TAR RNA Molecular Recognition Surface of the Tat Protein

MOLMOL views of Tat protein (pdb file 1TIV [20]) demonstrating that the basic region of the Tat protein forms a binding surface for the TAR RNA. Residues 52–57, which were identified here through EPR spectroscopy as important for the RNA-protein interfacial dynamics, are shown in green and form a single face of the binding surface. Residues 48–51, which were shown here to not affect TAR RNA interfacial dynamics, are shown in gold.

complex formation. More importantly, arginines 52 and 56 protrude into solution from the same side of the binding surface and likely form a platform for TAR RNA recognition. This observation, which indicates the importance of these residues for interfacial dynamics, provides indirect support for the EPR data identifying the importance of R56 in formation of the rigid complex. However, the final proof will be provided only by a high-resolution structure of the complex.

Significance

EPR spectroscopy was used to identify which amino acids in the basic region of the Tat protein are responsible for rigid TAR RNA-Tat protein molecular recognition. To our knowledge, this is the first example of using changes in RNA dynamics to investigate structural requirements for an RNA binding protein by EPR. Our results suggest arginines 52 and 56 were most important for rigid TAR-Tat complex formation, while the other C-terminal arginines 53, 55, and 57 contribute to specific binding to a lesser extent. In contrast, N-terminal residues were not important for complex formation. Furthermore, the results indicated that the overall TAR-Tat structure switched between a rigid state and a flexible state for complexes containing one of several C-terminal single point mutants. These results show the importance of specific contacts in the formation of a specific and rigid structure and provide further support for an induced-fit mechanism in the TAR RNA-Tat protein complex formation. This study highlights the utility of EPR spectroscopy for identifying critical residues in the formation of dynamic macromolecular complexes.

Experimental Procedures

Preparation of RNA

Unmodified and 2′-NH_2-modified RNAs were purchased from Dharmacon Research, Inc (Lafayette, CO). Spin-labeled RNAs were prepared as previously described by reaction of 4-isocyanato TEMPO with 2′-NH_2-modified RNA (Figure 1), followed by denaturing polyacrylamide gel purification [34, 37].

Purification of Tat-Derived Peptides

Peptides were purchased from United Biochemical Research, Inc. (Seattle, WA) and characterized by MALDI-TOF mass spectrometry. For EPR spectroscopy, small quantities (1–5 mg) were purified by RP-HPLC on a Beckman 421A HPLC using a Dynamax Rainin 300 Å 25 × 250 mm preparatory 5 μm C18 column. Sample elution was monitored by dual wavelength UV at 220 and 275 nm. Solvent gradients were run at 10 ml/min as follows: solvent A, 0.1% aq trifluoroacetic acid (TFA); solvent B, CH_3CN; 40-min linear gradient from 0% B to 50% B, 5 min linear gradient to 0% B. Collected samples were lyophilized to dryness and then dissolved in sterile water and quantified by UV spectroscopy at A_{275} (ϵ = 1420 l · mol^{-1} · cm^{-1}). It is critical to lyophilize the peptides to dryness; simple drying in a centrifuge in vacuo was insufficient to remove excess TFA, which subsequently denatured the RNA upon resuspension of the peptide solution and incubation with the TAR RNA.

EPR Spectroscopy

For CW-EPR, 2.0 nmol of spin-labeled RNA and 2.8 nmol of unmodified complement strand were incubated in 7.0 μl of 20% (w/v) aqueous sucrose/100 mM NaCl, 10 mM sodium phosphate, and 0.1 mM Na_2EDTA (pH 7.0) on a thermal cycler at 90°C for 2 min, 60°C for 5 min, 50°C for 5 min, 40°C for 5 min, and 22°C for 15 min. Tat-derived peptides in the above 20% aqueous sucrose phosphate buffer (3.0 μl) were then added to the above sample (final concentrations: 0.2 mM spin-labeled RNA, 0.5 mM peptide). RNA line samples were obtained in 0.8 × 1.0 mm quartz capillary (VitroCom, Inc.) and stored at 4°C between experiments. X-band (9.3 GHz) CW-EPR spectra were digitally recorded on a Bruker 300 EMX spectrometer equipped with a TE_{102} cavity. Samples were obtained at 273.2 ± 0.2 K. Experimental parameters included 3355 G center field, 100 kHz frequency modulation, 1.0 G modulation amplitude, 8 mW power, 20.48 ms time constant, 40.96 ms conversion, 1024 points, sweep time 42 s, and 110 G sweep width. Typically 100–300 scans were collected; the exact number depended on the signal to noise ratio, which was observed to be inversely proportional to the EPR spectroscopic width.

EPR Spectroscopic Analysis

EPR spectral widths ($2A_{zz}$) were measured directly from the spectra in WIN-EPR and span the crest of the low field peak (i.e., the outermost point where the slope of the spectrum is ~0) to the trough of the high field peak with an error between sample preparations as well as the measurement itself of 0.3 G (Figure 3). Spectra were further analyzed using MATLAB. The extent to which the rigid and flexible components were present in several multicomponent EPR spectra was determined by least squares optimization of the fit from the two component spectra. The spectra for the wild-type and mutant I peptides were used as the component spectra, and the

sum of the component spectra yielded a composite spectrum. Prior to summation, the individual component spectra were normalized to a unit area so that the coefficients could be interpreted in terms of fractional contribution to the composite spectra; to properly normalize the EPR spectra, the component spectra were scaled so that the double integral of each was unity. In addition to optimizing the coefficients of each component, the relative registration of each component on the abscissa with respect to the composite spectrum was allowed to vary. In practice, the amount that the spectrum was shifted along the *x* axis was never more than 3 Gauss.

Supplemental Data

Supplemental Data for this article is available online at http://www.chembiol.com/cgi/content/full/12/3/329/DC1/.

Acknowledgments

We thank the Sigurdsson research group, M. Hennig and G. Varani for critical review of this manuscript, T. Leeper for help in the preparation of Figure 7, the NIH for financial support (GM56947 and GM62360 to S.Th.S. and GM065944 to B.H.R.), and acknowledge a center grant from the National Institutes of Environmental Health Science/NIH (GM P30 ESO7033) for use of the EPR spectrometer. T.E.E. was supported by an NIH National Research Service Award (5 T32 GM08268).

Received: October 20, 2004
Revised: January 19, 2005
Accepted: January 20, 2005
Published: March 25, 2005

References

1. Frankel, A.D. (1992). Activation of HIV transcription by Tat. Curr. Opin. Genet. Dev. *2*, 293–298.
2. Yamaguchi, Y., Wada, T., and Handa, H. (1998). Interplay between positive and negative elongation factors: drawing a new view of DRB. Genes Cells *3*, 9–15.
3. Garber, M.E., Mayall, T.P., Suess, E.M., Meisenhelder, J., Thompson, N.E., and Jones, K.A. (2000). CDK9 autophosphorylation regulates high-affinity binding of the human immunodeficiency virus type 1 tat-P-TEFb complex to TAR RNA. Mol. Cell. Biol. *20*, 6958–6969.
4. Jones, K.A., and Peterlin, B.M. (1994). Control of RNA initiation and elongation at the HIV-1 promoter. Annu. Rev. Biochem. *63*, 717–743.
5. Froeyen, M., and Herdewijn, P. (2002). RNA as a target for drug design, the example of Tat-TAR interaction. Curr. Top. Med. Chem. *2*, 1123–1145.
6. Gallego, J., and Varani, G. (2001). Targeting RNA with small-molecule drugs: therapeutic promise and chemical challenges. Acc. Chem. Res. *34*, 836–843.
7. Roy, S., Delling, U., Chen, C.H., Rosen, C.A., and Sonenberg, N. (1990). A bulge structure in HIV-1 TAR RNA is required for Tat binding and Tat-mediated trans-activation. Genes Dev. *4*, 1365–1373.
8. Weeks, K.M., Ampe, C., Schultz, S.C., Steitz, T.A., and Crothers, D.M. (1990). Fragments of the HIV-1 Tat protein specifically bind TAR RNA. Science *249*, 1281–1285.
9. Weeks, K.M., and Crothers, D.M. (1991). RNA recognition by Tat-derived peptides: interaction in the major groove? Cell *66*, 577–588.
10. Sumner-Smith, M., Roy, S., Barnett, R., Reid, L.S., Kuperman, R., Delling, U., and Sonenberg, N. (1991). Critical chemical features in trans-acting-responsive RNA are required for interaction with human immunodeficiency virus type 1 Tat protein. J. Virol. *65*, 5196–5202.
11. Weeks, K.M., and Crothers, D.M. (1992). RNA binding assays for Tat-derived peptides: implications for specificity. Biochemistry *31*, 10281–10287.
12. Churcher, M.J., Lamont, C., Hamy, F., Dingwall, C., Green, S.M., Lowe, A.D., Butler, J.G., Gait, M.J., and Karn, J. (1993). High affinity binding of TAR RNA by the human immunodeficiency virus type-1 tat protein requires base-pairs in the RNA stem and amino acid residues flanking the basic region. J. Mol. Biol. *230*, 90–110.
13. Cordingley, M.G., LaFemina, R.L., Callahan, P.L., Condra, J.H., Sardana, V.V., Graham, D.J., Nguyen, T.M., LeGrow, K., Gotlib, L., Schlabach, A.J., et al. (1990). Sequence-specific interaction of Tat protein and Tat peptides with the transactivation-responsive sequence element of human immunodeficiency virus type 1 in vitro. Proc. Natl. Acad. Sci. USA *87*, 8985–8989.
14. Delling, U., Roy, S., Sumner-Smith, M., Barnett, R., Reid, L., Rosen, C.A., and Sonenberg, N. (1991). The number of positively charged amino acids in the basic domain of Tat is critical for trans-activation and complex formation with TAR RNA. Proc. Natl. Acad. Sci. USA *88*, 6234–6238.
15. Calnan, B.J., Tidor, B., Biancalana, S., Hudson, D., and Frankel, A.D. (1991). Arginine-mediated RNA recognition: the arginine fork. Science *252*, 1167–1171.
16. Tao, J., and Frankel, A.D. (1992). Specific binding of arginine to TAR RNA. Proc. Natl. Acad. Sci. USA *89*, 2723–2726.
17. Tao, J., and Frankel, A.D. (1993). Electrostatic interactions modulate the RNA-binding and transactivation specificities of the human immunodeficiency virus and simian immunodeficiency virus Tat proteins. Proc. Natl. Acad. Sci. USA *90*, 1571–1575.
18. Calnan, B.J., Biancalana, S., Hudson, D., and Frankel, A.D. (1991). Analysis of arginine-rich peptides from the HIV Tat protein reveals unusual features of RNA-protein recognition. Genes Dev. *5*, 201–210.
19. Aboul-ela, F., Karn, J., and Varani, G. (1996). Structure of HIV-1 TAR RNA in the absence of ligands reveals a novel conformation of the trinucleotide bulge. Nucleic Acids Res. *24*, 3974–3981.
20. Bayer, P., Kraft, M., Ejchart, A., Westendorp, M., Frank, R., and Rosch, P. (1995). Structural studies of HIV-1 Tat protein. J. Mol. Biol. *247*, 529–535.
21. Peloponese, J.M., Jr., Gregoire, C., Opi, S., Esquieu, D., Sturgis, J., Lebrun, E., Meurs, E., Collette, Y., Olive, D., Aubertin, A.M., et al. (2000). ^{1}H-^{13}C nuclear magnetic resonance assignment and structural characterization of HIV-1 Tat protein. C. R. Acad. Sci. III *323*, 883–894.
22. Gregoire, C., Peloponese, J.M., Jr., Esquieu, D., Opi, S., Campbell, G., Solomiac, M., Lebrun, E., Lebreton, J., and Loret, E.P. (2001). Homonuclear (1)H-NMR assignment and structural characterization of human immunodeficiency virus type 1 Tat Mal protein. Biopolymers *62*, 324–335.
23. Puglisi, J.D., Chen, L., Frankel, A.D., and Williamson, J.R. (1993). Role of RNA structure in arginine recognition of TAR RNA. Proc. Natl. Acad. Sci. USA *90*, 3680–3684.
24. Puglisi, J.D., Tan, R., Calnan, B.J., Frankel, A.D., and Williamson, J.R. (1992). Conformation of the TAR RNA-arginine complex by NMR spectroscopy. Science *257*, 76–80.
25. Aboul-ela, F., Karn, J., and Varani, G. (1995). The structure of the human immunodeficiency virus type-1 TAR RNA reveals principles of RNA recognition by Tat protein. J. Mol. Biol. *253*, 313–332.
26. Brodsky, A.S., and Williamson, J.R. (1997). Solution structure of the HIV-2 TAR-argininamide complex. J. Mol. Biol. *267*, 624–639.
27. Hennig, M., and Williamson, J.R. (2000). Detection of N-H...N hydrogen bonding in RNA via scalar couplings in the absence of observable imino proton resonances. Nucleic Acids Res. *28*, 1585–1593.
28. Pitt, S.W., Majumdar, A., Serganov, A., Patel, D.J., and Al-Hashimi, H.M. (2004). Argininamide binding arrests global motions in HIV-1 TAR RNA: comparison with Mg(2+)-induced conformational stabilization. J. Mol. Biol. *338*, 7–16.
29. Long, K.S., and Crothers, D.M. (1999). Characterization of the solution conformations of unbound and Tat peptide-bound forms of HIV-1 TAR RNA. Biochemistry *38*, 10059–10069.
30. Hubbell, W.L., Gross, A., Langen, R., and Lietzow, M.A. (1998). Recent advances in site-directed spin labeling of proteins. Curr. Opin. Struct. Biol. *8*, 649–656.

31. Hubbell, W.L., Cafiso, D.S., and Altenbach, C. (2000). Identifying conformational changes with site-directed spin labeling. Nat. Struct. Biol. *7*, 735–739.
32. Columbus, L., and Hubbell, W.L. (2002). A new spin on protein dynamics. Trends Biochem. Sci. *27*, 288–295.
33. Qin, P.Z., and Dieckmann, T. (2004). Application of NMR and EPR methods to the study of RNA. Curr. Opin. Struct. Biol. *14*, 350–359.
34. Edwards, T.E., Okonogi, T.M., and Sigurdsson, S.T. (2002). Investigation of RNA-protein and RNA-metal ion interactions by electron paramagnetic resonance spectroscopy. The HIV TAR-Tat motif. Chem. Biol. *9*, 699–706.
35. Edwards, T.E., and Sigurdsson, S.T. (2003). EPR spectroscopic analysis of TAR RNA-metal ion interactions. Biochem. Biophys. Res. Commun. *303*, 721–725.
36. Edwards, T.E., and Sigurdsson, S.T. (2002). Electron paramagnetic resonance dynamic signatures of TAR RNA-small molecule complexes provide insight into RNA structure and recognition. Biochemistry *41*, 14843–14847.
37. Edwards, T.E., Okonogi, T.M., Robinson, B.H., and Sigurdsson, S.T. (2001). Site-specific incorporation of nitroxide spin-labels into internal sites of the TAR RNA; structure-dependent dynamics of RNA by EPR spectroscopy. J. Am. Chem. Soc. *123*, 1527–1528.
38. Qin, P.Z., Butcher, S.E., Feigon, J., and Hubbell, W.L. (2001). Quantitative analysis of the isolated GAAA tetraloop/receptor interaction in solution: a site-directed spin labeling study. Biochemistry *40*, 6929–6936.
39. Qin, P.Z., Hideg, K., Feigon, J., and Hubbell, W.L. (2003). Monitoring RNA base structure and dynamics using site-directed spin labeling. Biochemistry *42*, 6772–6783.
40. Kim, N.K., Murali, A., and DeRose, V.J. (2004). A distance ruler for RNA using EPR and site-directed spin labeling. Chem. Biol. *11*, 939–948.
41. Fanucci, G.E., Cadieux, N., Kadner, R.J., and Cafiso, D.S. (2003). Competing ligands stabilize alternate conformations of the energy coupling motif of a TonB-dependent outer membrane transporter. Proc. Natl. Acad. Sci. USA *100*, 11382–11387.
42. Bhargava, K., and Feix, J.B. (2004). Membrane binding, structure, and localization of cecropin-mellitin hybrid peptides: a site-directed spin-labeling study. Biophys. J. *86*, 329–336.
43. Hurth, K.M., Nilges, M.J., Carlson, K.E., Tamrazi, A., Belford, R.L., and Katzenellenbogen, J.A. (2004). Ligand-induced changes in estrogen receptor conformation as measured by site-directed spin labeling. Biochemistry *43*, 1891–1907.
44. Columbus, L., and Hubbell, W.L. (2004). Mapping backbone dynamics in solution with site-directed spin labeling: GCN4–58 bZip free and bound to DNA. Biochemistry *43*, 7273–7287.
45. Freed, J.H. (1976). Theory of slow tumbling ESR spectra for nitroxides. In Spin Labeling: Theory and Application, L.J. Berliner, ed. (New York: Academic Press), pp. 53–132.
46. Allen, M., Varani, L., and Varani, G. (2001). Nuclear magnetic resonance methods to study structure and dynamics of RNA-protein complexes. Methods Enzymol. *339*, 357–376.
47. Xia, T., Becker, H.C., Wan, C., Frankel, A., Roberts, R.W., and Zewail, A.H. (2003). The RNA-protein complex: direct probing of the interfacial recognition dynamics and its correlation with biological functions. Proc. Natl. Acad. Sci. USA *100*, 8119–8123.
48. Brodsky, A.S., Erlacher, H.A., and Williamson, J.R. (1998). NMR evidence for a base triple in the HIV-2 TAR C-G.C+ mutant-argininamide complex. Nucleic Acids Res. *26*, 1991–1995.
49. Zacharias, M., and Hagerman, P.J. (1995). The bend in RNA created by the trans-activation response element bulge of human immunodeficiency virus is straightened by arginine and by Tat-derived peptide. Proc. Natl. Acad. Sci. USA *92*, 6052–6056.
50. Dayie, K.T., Brodsky, A.S., and Williamson, J.R. (2002). Base flexibility in HIV-2 TAR RNA mapped by solution (15)N, (13)C NMR relaxation. J. Mol. Biol. *317*, 263–278.
51. Long, K.S., and Crothers, D.M. (1995). Interaction of human immunodeficiency virus type 1 Tat-derived peptides with TAR RNA. Biochemistry *34*, 8885–8895.
52. Xie, B., Wainberg, M.A., and Frankel, A.D. (2003). Replication of human immunodeficiency viruses engineered with heterologous Tat-transactivation response element interactions. J. Virol. *77*, 1984–1991.
53. Xie, B., Calabro, V., Wainberg, M.A., and Frankel, A.D. (2004). Selection of TAR RNA-binding chameleon peptides by using a retroviral replication system. J. Virol. *78*, 1456–1463.